Sensitivities of the Proton-Nucleus Elastic Scattering Observables of ^{6}He and ^{8}He at Intermediate Energies

S.P. Weppner and Ofir Garcia

Natural Sciences, Eckerd College, St. Petersburg, Florida 33711

Ch. Elster

Institute of Nuclear and Particle Physics, Ohio University, Athens, Ohio 45701

(January 17, 2000)

We investigate the use of proton-nucleus elastic scattering experiments using secondary beams of ^{6}He and ^{8}He to determine the physical structure of these nuclei. The sensitivity of these experiments to nuclear structure is examined by using four different nuclear structure models with different spatial features using a full-folding optical potential model. The results show that elastic scattering at intermediate energies (< 100 MeV per nucleon) is not a good constraint to be used to determine features of structure. Therefore researchers should look elsewhere to put constraints on the ground state wave function of the ^{6}He and ^{8}He nuclei.

I. INTRODUCTION

The advent of radioactive accelerator beams during the past decade has enhanced the variety of nuclear reactions available for study. In the present research we concentrate on the neutron rich isotopes of helium, ^{6}He and ^{8}He, which have been produced as secondary beams at intermediate energies [1,2]. The simplified shell model structure of these isotopes is thought to be a core ^{4}He, surrounded by loosely bound valence neutrons located in the p shell, denoted often as the nuclear halo. A significant amount of research has been done on constructing models that reproduce data from experimental reactions involving these isotopes (Refs. [3–8], [9–16] [17–22] for example). To use radioactive beams effectively in nuclear studies the present uncertainty in the ground state wave functions of ^{6}He and ^{8}He must be reduced. Once the wave functions are known with better precision, the radioactive beam experiments may produce significant implications for neutron stars, shell model calculations, the two body nuclear force, and the three body nuclear force.

One way to ascertain the physical structure of the exotic helium nuclei would be to use elastic scattering data. We want to address the feasibility of this method by developing proton-^{6}He and proton-^{8}He first order optical potentials at intermediate energies (60 MeV-100 MeV per nucleon) using different structure models as inputs to this optical potential model. A fair amount of earlier work examines this sensitivity [4–7], [8–13,23], but there is not full agreement in the literature on the strength of this sensitivity of structure to elastic scattering data. For example Ref. [5] found that at these energies proton-nucleus elastic scattering data was not an effectual tool in determining structure. Korsheninnikov *et al.* [11,12] also did a detailed study on the sensitivities of proton elastic scattering not only of the helium isotopes but also the lithium isotopes (^{9}Li and ^{11}Li), using an eikonal approach. They concluded that elastic scattering "is not a very promising tool" to determine structure of the valence neutrons. Their belief is that the size of the core plays a more important role in determining the differential cross section than the lower density valance neutrons. More recently, and in contrast, Karataglidas *et al.* [13] have performed calculations on the same exotic helium reactions at intermediate energy range using a few different variations of a structure calculation in a g-matrix elastic optical potential calculation. They concluded for ^{6}He that the data available was insufficient for the elastic scattering calculations to discern the existence of a halo. For ^{8}He, they ascertained that there was enough data to conclude that it is not a halo nucleus from comparing differences in the elastic differential cross section calculations.

In the literature there is not general agreement to the question of sensitivity of the elastic proton-nucleus differential cross section at intermediate energies to the structure calculation of the target nuclei ^{6}He and ^{8}He. Most research concludes that the sensitivity is not there to determine structure, but some authors have used elastic proton-nucleus scattering to put constraints on the details of their physical structure, specifically the halo. In this work, we will systematically examine this sensitivity using four independent structure models and conclude whether elastic scattering is a tool that should be used to ascertain the structure of ^{6}He and ^{8}He.

In section II, we will briefly summarize our full-folding optical potential calculation technique which we use to describe elastic proton-^{6}He and proton-^{8}He scattering and we outline the four different structure models used to describe the helium isotopes. Our results are in section III and our conclusions are in section IV.

II. FULL-FOLDING OPTICAL POTENTIAL

A standard microscopic approach to the elastic scattering of a strongly interacting projectile from a target

of A particles is given by the formulation of an optical potential in '$\tau\rho$' form where τ contains information about the nucleon-nucleon interaction and ρ is a nuclear structure calculation (ground state density) of the target. The development of this optical potential begins with the separation of the Lippmann-Schwinger equation for the transition amplitude

$$T = V + VG_0(E)T \qquad (1)$$

into two parts, namely an integral equation for T:

$$T = U + UG_0(E)PT, \qquad (2)$$

where U is the optical potential operator given through a second integral equation

$$U = V + VG_0(E)QU. \qquad (3)$$

In the above equations, the potential operator V represents the external many-body interaction. The potential operator $V = \sum_{i=1}^{A} v_{0i}$ consists of the two-body potential v_{0i} acting between the projectile and the nucleons in the target nucleus. The operators P and Q are projection operators, $P + Q = 1$, and P is defined such that Eq. (2) is solvable. In this case, P is conventionally taken to project onto the elastic channel. For more details see Refs. [24,25].

The evaluation of the full-folding optical potential requires a fully off-shell nuclear density matrix, which in its most general form is given as

$$\rho(\mathbf{r}', \mathbf{r}) = \Phi_A^{\dagger}(\mathbf{r}') \, \Phi_A(\mathbf{r}). \qquad (4)$$

Here, $\Phi_A(\mathbf{r})$ is the wave function describing the nuclear ground state in position space. We choose four models for this work to describe the ^{6}He and ^{8}He ground state. The structure models vary in rigor, quality, and applicability in describing these exotic helium nuclei. First, a general description of each model will be given in part A, to be followed by comparisons of all four models in part B.

A. Descriptions of the four off-shell densities

Our first model, proposed by Sherr [26], will be referred to as the 'boot-strap' model (BS). This model was created to describe the root mean squared (rms) radii of a variety of exotic nuclei using a simple description of the nucleus. It represents the valence neutrons by using a Woods-Saxon potential which is fit to the two neutron binding energy. It then follows a sequential step procedure to build the exotic nuclei. Explicitly for helium, the model starts with the well known core ^{4}He, and then builds ^{6}He by calculating the wave function for the valence neutrons. Likewise, to construct ^{8}He, ^{6}He is considered the core and the 2 neutron wave function generated from a Woods-Saxon potential is calculated. Wave

functions for the ^{4}He core and valence neutrons were calculated in r space (relative to the center of mass of the whole nucleus), then Fourier transformed to momentum space

$$\rho'(\mathbf{p}', \mathbf{p}) = \frac{1}{8\pi^3} \int d^3\mathbf{r}' e^{-i\mathbf{r}' \cdot \mathbf{p}'} \int d^3\mathbf{r} e^{-i\mathbf{r} \cdot \mathbf{p}} \, \rho(\mathbf{r}', \mathbf{r}), \quad (5)$$

where they were used in construction of the off-shell density via Eq. (4). The validity of this model is questionable due to its extreme simplicity. It is thought that the size of the ^{4}He core in the exotic isotopes is larger than the bare ^{4}He radius which this model assumes [20]. The mode of construction of ^{8}He is also in contradiction with most other structure calculations for ^{8}He. To first order, ^{6}He could be approximated as a ^{4}He + 2n; however, it is apparent that ^{8}He is closer to ^{4}He+4n than (^{4}He +2n) +2n as the BS model would suggest [20].

The second model is a relativistic point coupling model within the framework of a chiral effective field theory by Rusnak and Furnstahl [27]. A Lagrangian is constructed: an expansion in powers of the scalar, vector, isovector-vector, tensor, and isovector-tensor densities, and their derivatives. The theory contains all the symmetries of QCD and is able to calculate low energy features, such as the structure of nuclei ground states adequately. For this paper, we used what Ref. [27] refers to as the 'FZ4' scheme. Here, the vector meson and ρ meson masses are fixed, while the coefficients of the densities to fourth order are varied to produce a low chi-square to experimental observables. Most varieties of the chiral effective theory reproduce the bulk nuclear observables of spherically symmetric nuclei. Questions of applicability to exotic helium nuclei can of course be raised while using this model, for it was not developed for the non-spherical, non-bulk nuclei ^{6}He and ^{8}He. The numerical procedure to create the off-shell densities (Eq. 4) used for the optical potential is given in Ref. [24].

The third nuclear structure model used to describe the densities ^{6}He and ^{8}He, a Dirac-Hartree model (DH) [30,31], has been used extensively by two of the authors (Ch. Elster and S. P. Weppner) to describe the structure of doubly magic spherical nuclei with success [24,25,32–35]. This is the oldest structure model of the four models discussed. The FZ4 model (detailed above) has the same structure wave function, so the method used to create the momentum off-shell density of Eq. (4) is the same for both models and is detailed in Refs. [24,25]. Applicability is a concern for this model also. When developed, it was fit to the bulk properties of ^{16}O, ^{40}Ca, ^{48}Ca, ^{90}Zr, and ^{208}Pb, all doubly magic nuclei. Furthermore, this model, as well as FZ4, falls under the mean field ansatz, which is rather tenable when describing nuclei with only 6 or 8 nucleons. It was also developed well before the general structure of ^{6}He and ^{8}He were apparent, thereby making it a candidate to test whether the elastic observables can detect this non-applicability.

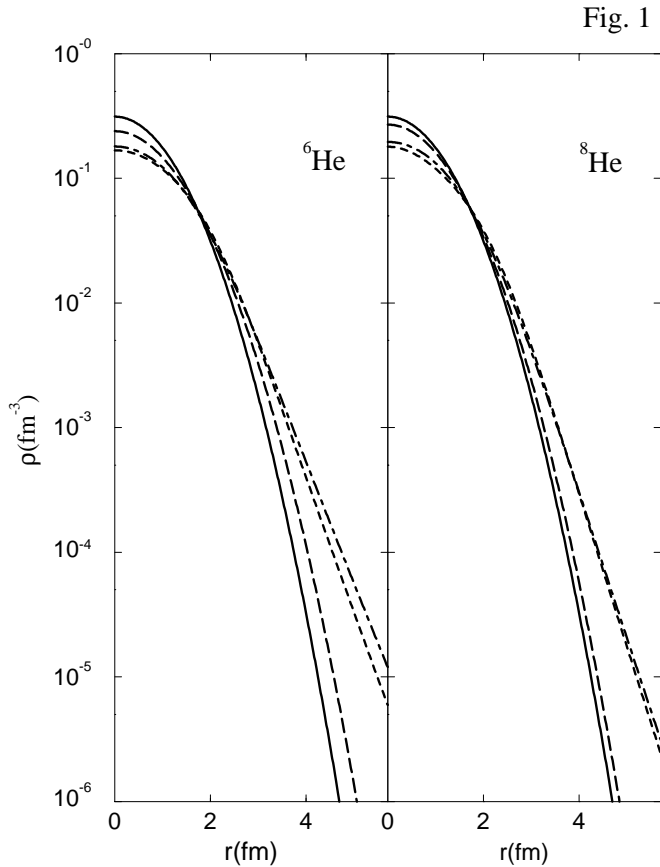FIG. 1. Proton density calculations in position space for ^{6}He and ^{8}He. The solid line represents the calculation performed with a Boot Strap nuclear structure model [26]. The short dashed line represents the same calculation using a chiral model [27,28] for the nuclear structure. The dash-dotted line represents the same calculation using a Dirac-Hartree model [30,31] as the nuclear structure calculation and the long dashed line has a cluster orbit shell model approximation (COSMA) [20,21] as a model.

FIG. 2. The legend is the same as Fig. 1 except the lines now represent calculations of neutron densities.

The last nuclear model to be discussed was developed explicitly for exotic nuclei. The COSMA model (cluster orbit shell model approximation) [20,21], an approximation to the three body problem, has been used extensively in the literature to describe elastic scattering with the exotic helium nuclei [4,6,7,11,12,36,40]. The COSMA model is a combination of nucleon clustering and the standard shell model, which obeys the Pauli exclusion principle by using Slater determinants to produce a fully antisymmetrized wave function in r-space. They are then translated as single particle wave functions relative to the center of mass of the entire nucleus. These wave functions are Fourier transformed into momentum space using the method of Eq. (5), thus making it possible to create a fully off-shell density in momentum space.

There have been more rigorous models developed for ^{6}He and ^{8}He (Refs. [2,17–20,37] among others) which we have not used. In all cases, these models treat the three body problem (core + nucleon + nucleon) or (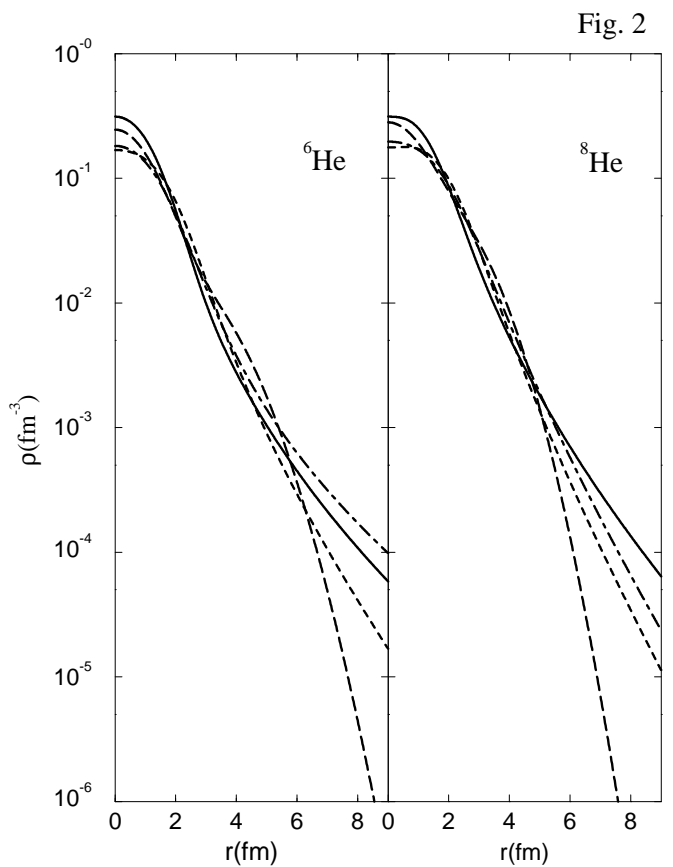core +di-neutron +di-neutron) with fewer approximations than the models presented here. Our goal is to present a sensitivity test, rather than produce the most fundamental calculations possible. To that end, we have used four highly varying models, with different characteristics, which are easy to calculate. As an aside, in a comparison between a realistic three body approach (treating the antisymmetry correctly) and the reducible two body approximation, the authors of Ref. [37] note little difference at intermediate and long ranges. They do find small differences in the short range behavior of the wave functions, but these are of little consequence when describing intermediate energy elastic scattering. Therefore we would expect our results using these simpler models to differ little from results using the more rigorous realistic models.

B. Nuclear structure of the four models

In Fig. 1, we have plotted the proton densities in r-space of all four structure models described above. The general characterization is that the core two protons and two neutrons are more tightly bound in the two models that are designed for exotic nuclei, these being the BS model (solid line) and COSMA model (long dashed line). These models have a core close to that of the lone ^{4}He nucleus (≈ 1.6 fm). In contrast, the FZ4 model (short

^{6}He								
Model	r_{rms} [fm]	r_c [fm]	Δr_c [fm]	r_v [fm]	Δr_v [fm]	S_{2n} [MeV]	S_d [fm]	halo?
BS	2.90	1.61	0.63	4.47	2.59	0.98	-0.36	no
FZ4	2.54	1.98	0.81	3.39	1.52	1.80	-0.92	no
DH	3.75	2.00	0.84	5.84	3.49	0.19	-0.49	no
COSMA	2.57	1.77	0.69	3.68	1.20	–	+0.02	yes
EXP	2.39	–	–	–	–	0.97	?	?
^{8}He								
Model	r_{rms} [fm]	r_c [fm]	Δr_c [fm]	r_v [fm]	Δr_v [fm]	S_{4n} [MeV]	S_d[fm]	halo?
BS	2.84	1.61	0.63	3.68	1.91	3.12	-0.47	no
FZ4	2.57	1.95	0.80	3.08	1.24	3.47	-0.91	no
DH	2.75	1.90	0.79	3.39	1.41	2.68	-0.71	no
COSMA	2.52	1.69	0.66	3.14	0.99	–	-0.20	no
EXP	2.49	–	–	–	–	3.1	?	?

TABLE I. Comparison of the four structure models observables with each other and experiment. The root mean squared matter (rms) radius (r_{rms}) of the whole nucleus, the rms radius of the two neutron-two proton core wave function(r_c), the standard deviation of the core (Δr_c), the valence neutron matter radius (r_v), the standard deviation of the valence neutron wave function (Δr_v), the separation energy of the valence neutrons (S_{2n}), the separation distance of one standard deviation of the core and valence wave functions (S_d), and a statement on whether the model has a halo structure as defined by this work. The experimental results are from Ref. [42].

dashed line) and the DH model (dashed-dotted line) have a core which ranges from 12% to 20% larger than their exotic counterparts.

The total neutron densities in r-space have also been plotted for all four structure models for ^{6}He and ^{8}He in Fig. 2. Comparing the exotic nuclei structure models first, the BS model (solid line) and COSMA model (long dashed line) have a tight two-neutron core because their densities are higher in the 0 fm to 2 fm range. At about 3 fm, differences begin to emerge between these two exotic models. All models do have an extended neutron wave function of varying degrees, with the COSMA model having the most unique shape.

In Table I, we list the four models and the characteristics they describe. All position measurements are relative to the center of mass of the ^{6}He or ^{8}He system. Calculated in Table I are the root mean squared matter radius (r_{rms}) of the whole nucleus, the rms radius of the two neutron-two proton core wave function(r_c), the standard deviation of the core (Δr_c), the valence neutron matter radius (r_v), the standard deviation of the valence neutron wave function (Δr_v), the separation energy of the valence neutrons, the separation distance of one standard deviation of the core and valence wave functions, and a statement on whether the model has a halo structure as defined by this work. The definition of the standard deviation is

$$\Delta r = \sqrt{<r^2> - <r>^2}, \quad (6)$$

whereas the separation distance is defined as

$$S_d = r_v - \Delta r_v - \Delta r_c - r_c. \quad (7)$$

Simply if $S_d > 0$ then we define this nucleus as having a halo because there is a well defined separation between the core and halo centers. The only discernible

halo nucleus is the COSMA model of ^{6}He. It contains a tightly bounded core wave function with adequate spacing between core and valence nucleons. The COSMA model also has a significantly different asymptotic wave function shape. The other three models do not define a halo for the ^{6}He nucleus, as there is too much significant overlap between the core and valence wave functions. No model produces a definitive halo for ^{8}He, although COSMA comes closest.

In summary it is concluded that the most disparate structure is the COSMA model. One would expect that because this model is used often to describe exotic nuclei, it should also best describe elastic scattering if the observables are sensitive to the nuclear structure calculation. In the next section we will use these four models as input into our optical potential to describe elastic scattering at the intermediate energy range.

III. RESULTS AND DISCUSSION

The elastic scattering of protons from ^{6}He and ^{8}He at incident proton energies from 66 MeV to 100 MeV are calculated. At this energy range, the proton-nucleus elastic scattering data are scarce and exist only at forward angles. We will focus on the reactions where experimental data for the elastic differential cross-sections exists, but we will also comment on how our conclusions would change if the experimental database were enlarged. Other observables which are calculated in this work, for which no data exists, are the spin rotation function (Q) and the analyzing power (A_y). We will also comment on sensitivity to these observables.

The full-folding optical potential used for these results is calculated as outlined in Refs. [24,25], and we use the
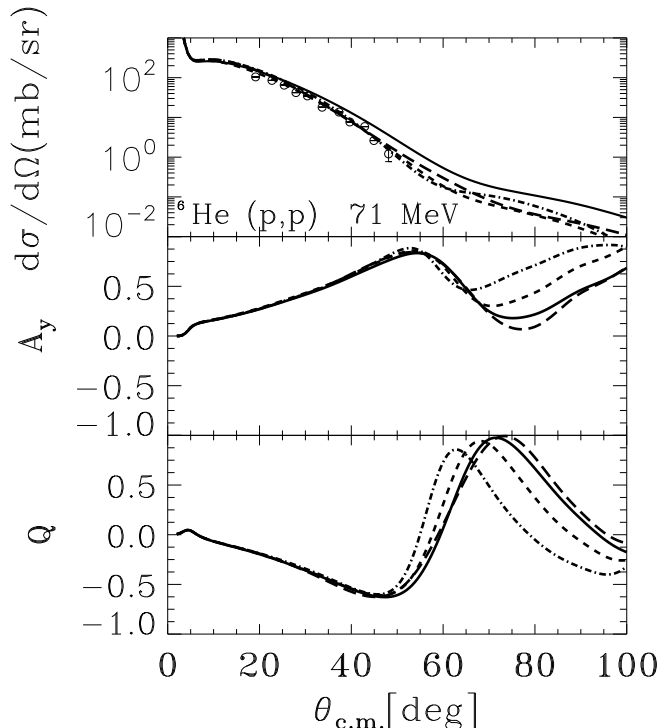
FIG. 3. The angular distribution of the differential cross-section ($\frac{d\sigma}{d\Omega}$), analyzing power (A_y) and spin rotation function (Q) are shown for elastic proton scattering from ^{6}He at 71 MeV laboratory energy. All calculations are denoted with the same legend as Fig. 1. The solid line represents the calculation performed with a first-order full-folding optical potential using the Boot Strap nuclear structure model [26] as an input to the optical potential. The short dashed line represents the same calculation using a chiral model [27,28] for the nuclear structure of ^{6}He. The dash-dotted line represents the same calculation using a Dirac-Hartree model [30,31] as the nuclear structure calculation and the long dashed line has a cluster orbit shell model approximation (COSMA) [20,21] as a model. All calculations use Nijmegen I for their NN interaction [38]. The data (circles) are taken from Ref. [1].

FIG. 4. Same as Fig. 3, except that the reaction is a proton at 66 MeV laboratory energy elastically scattering from ^{8}He. The data are taken from Ref. [1].

A. Elastic scattering results: effects of structure

The scattering observables for elastic proton scattering from ^{6}He at 71 MeV are displayed in Fig. 3. There are four calculations on the figure (using the same legend as Figs. 1-2). The solid line represents the elastic differential cross-section calculated from a full-folding optical potential using the BS model as the structure calculation, and the short-dashed line represents a calculation of the observables from a full-folding optical potential using the FZ4 model as the structure calculation. The DH version of the calculation is represented by the dot-dashed line while the optical potential using the COSMA structure model was used in the calculation of the long-dashed line. All models use the Nijmegen I nucleon-nucleon interaction. The experimental data for this reaction were given in Ref. [1]. As also seen in Fig. 1, the only calculation which does not adequately describe the limited experimental data for this reaction is the BS model. Referring to Table I, the only significant difference between this model and other models is the extremely small core which mimics the size of a lone ^{4}He nucleus. The other three models agree favorably with the limited data, yet when one looks at their features there are large differences in their binding energies, rms radii, and presence of a discernible halo. Therefore, it is impossible to draw any conclusions about the structure of ^{6}He valance neutrons from this reaction. We may draw some inferences on the appropriate size of the core from looking at the

four model densities as described in Sec. II. We will refer to the model of Ref. [26] as 'BS'. The Dirac-Hartree model of Refs. [30,31] will be labeled 'DH'. The chiral point coupling model of Ref. [27,28] will be labeled 'FZ4'. The cluster model of Refs. [20,21] will be referred to as 'COSMA'.

The full-folding optical potential also requires a model of the NN interaction. In this work, we use the Nijmegen I interaction [38]. We have also calculated some optical potentials using the CD Bonn NN potential [39]. This potential has the same tight constraints of the Nijmegen for its on shell values to agree with np and pp data, but the off shell amplitudes are different. The elastic scattering calculations using the CD Bonn potential show very little difference with those that use the Nijmegen potential. The conclusions drawn in this work are therefore independent of the choice of which modern NN potential was used.
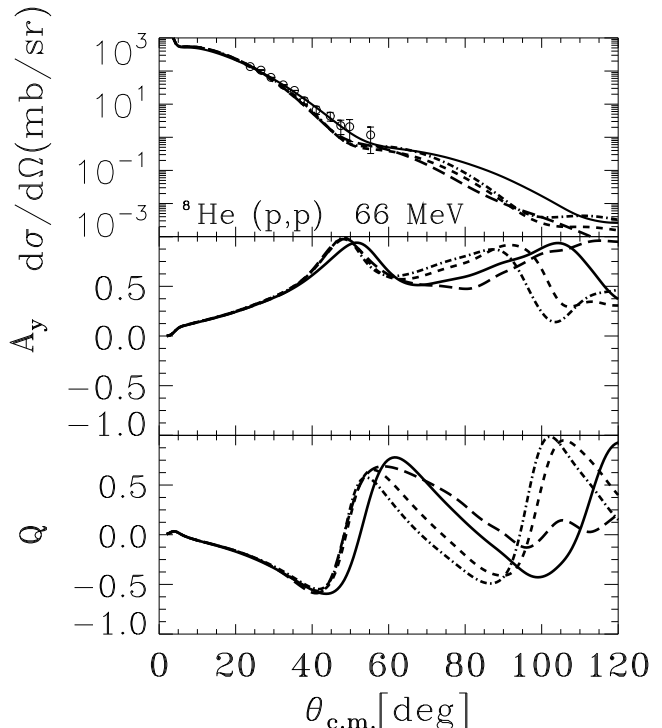
Fig. 5　　　　　　　　　　　　　　　　　　　　Fig. 6
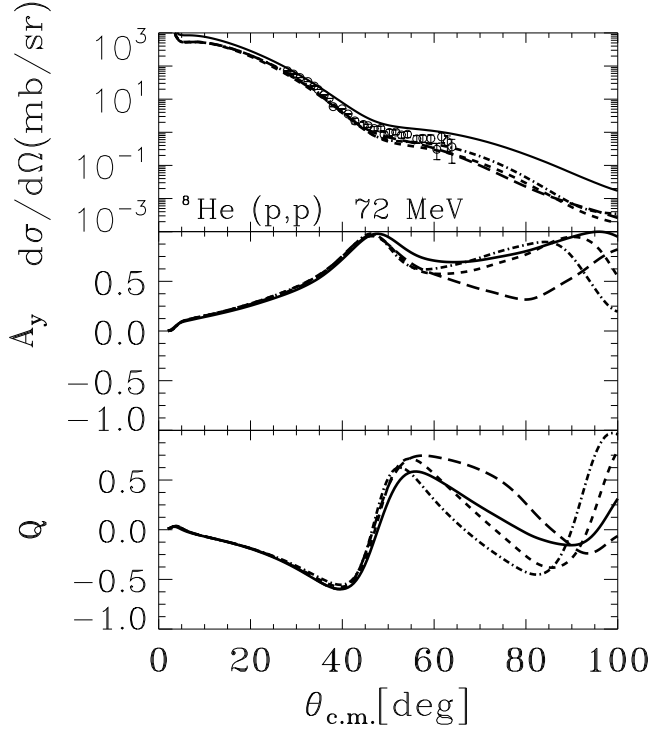

FIG. 5. Same as Fig. 3, except that the reaction is a proton at 72.5 MeV laboratory energy elastically scattering from ^{8}He. The data are taken from Ref. [2].

FIG. 6. Same as Fig. 3, except that the reaction is a proton at 100 MeV laboratory energy elastically scattering from ^{8}He. No data exists for this reaction.

results produced using the BS model, but the shape and existence of a halo cannot be determined from this reaction.

In Fig. 4, we calculate elastic scattering from ^{8}He at a projectile energy of 66 MeV. The legend represents the same calculations as in Fig. 3. The experimental data are from Ref. [1]. All four models adequately represent the data. The one model with the most significant differences in shape is again the BS model (and only at higher angles). This model has the tightest core, and a loose valence wave function, as it had for ^{6}He. There is nothing that can be learned about the valance structure of ^{8}He from studying this reaction's differential cross section for the data which exist. Polarization measurements (specifically Q) may be used if polarized experiments are done at large angles to high accuracy ($>60^o$).

We move to a slightly higher projectile energy in Fig. 5, where protons are scattered from ^{8}He at a projectile energy of 72.5 MeV. Again, the calculations have the same legend as given in Figs. 3 and Fig. 4. The data for this calculation are the most extensive in this energy range, they approach the 65° center of mass angle. Unfortunately the structure of ^{8}He still cannot be determined from this experiment. The sensitivities due to the structure calculation are not strong enough, given the experimental error, to ascertain the structure of ^{8}He. According to Table I, the COSMA model has a more defined valence ring than the others, but the differential cross section experimental data are unable to differentiate the validity of any of these disparate models unless experimenters were able
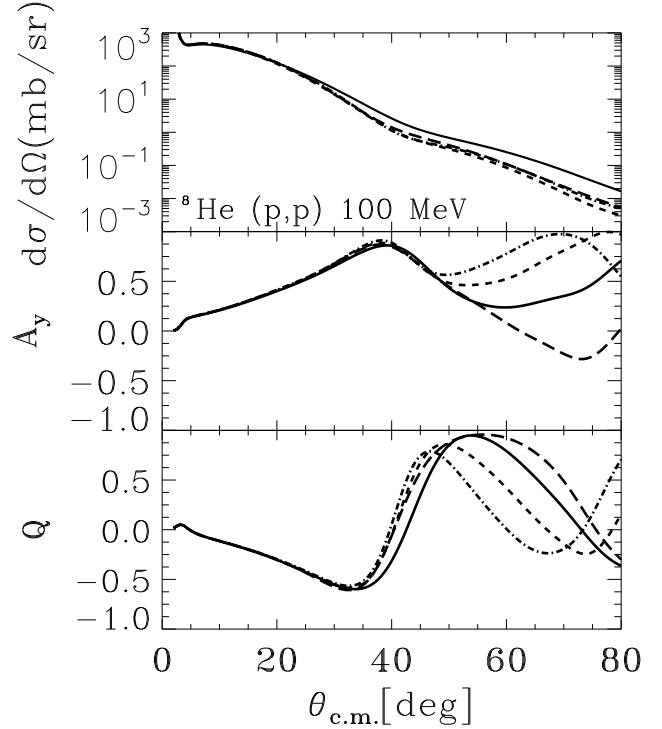
to measure the differential cross-section with a margin of error of less than 20% at angles above 65°.

In Fig. 6, we explore a higher energy reaction where no experimental data exist. Here, we calculated protons scattering from ^{8}He at 100 MeV. Once more, the calculations use the same models and line definitions as in Figs. 3-5. Again, the three structure calculations give similar results (DH,FZ4, COSMA). The BS model runs high through the whole calculation, similar in significance to the previous figures. Polarization experiments also tell us little below 70° scattering center of mass angle. Even at 100 MeV the elastic reaction is insensitive to the structure of the valence neutrons in ^{8}He.

Recently, in Ref. [13], a similar study was done using these elastic reactions and pion production. The authors concluded that neither ^{6}He nor ^{8}He were halo nuclei. Their inclusion of a halo in their structure calculations always lowered the differential cross section at angles greater than 15°. In this present work, we did not find such a simple relationship between non-halo and halo nuclei. In fact, the most extreme halo model of ^{6}He (dashed line - COSMA) was not at either extreme of the differential cross section calculation of Fig. 5. We therefore conclude that the differential cross section is only slightly sensitive to the existence of a halo (S_d), the spread of the halo (Δr_v), the radius of the core nucleons (r_c), and the binding energy of the core nucleons (Δr_c), all of which are coupled to each other in a complex fashion. The structure parameter that seems to have the most influence at this energy is the radius of the core ^{4}He
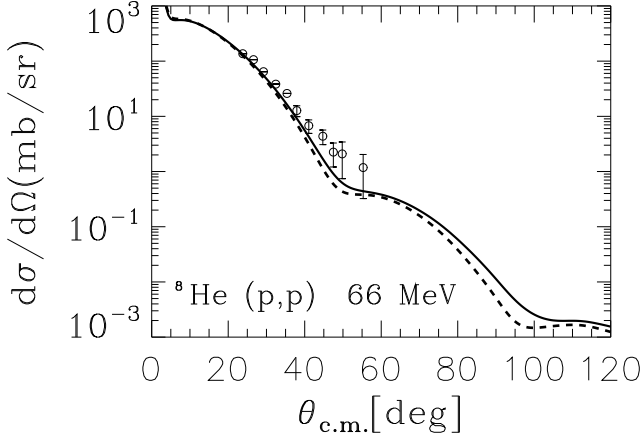
Fig. 7

Fig. 8

FIG. 7. The angular distribution of the differential cross-section ($\frac{d\sigma}{d\Omega}$) is shown for elastic proton scattering from ^{8}He at 66 MeV laboratory energy. The solid line is a calculation without medium effects, the short dashed line has medium effects included. Both calculations use a chiral model [27,28] for the nuclear structure calculation of ^{8}He and use the Nijmegen I potential [38] as their NN interaction. The data (circles) are taken from Ref. [1].
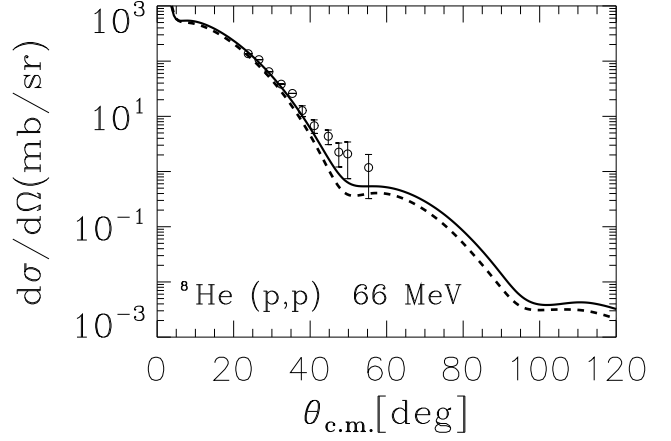
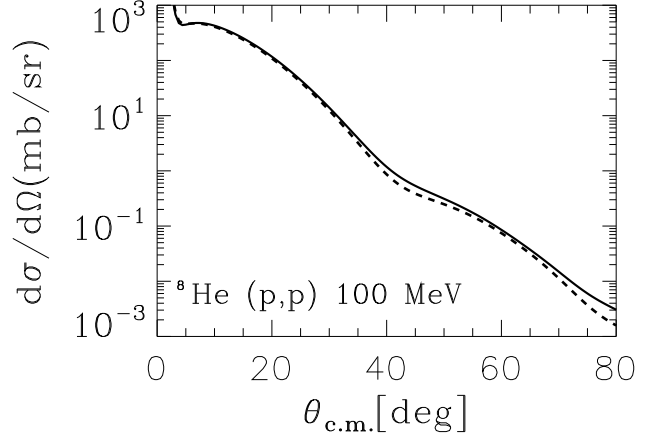FIG. 8. Same as Fig. 7, except both calculations use a Dirac Hartree calculation [30,31] to model ^{8}He.

Fig. 9

FIG. 9. Same as Fig. 7, except that now the reaction is at 100 MeV laboratory energy. There is no data for this reaction.

particle. There seems to be almost complete insensitivity to the valence neutron wave functions. To reiterate, the COSMA model has a very distinct asymptotic shape for the valence neutrons, and this uniqueness does not transfer into the differential cross section as exhibited by the similarity in the calculations.

B. Medium effects

So far in this work, we have used the impulse approximation, setting the medium field to zero. In previous work two of the authors (Ch. Elster and S. P. Weppner) showed that at 65 MeV, if a medium field was used (as outlined briefly in Section II, and in more detail in Refs. [32,33,35]) then there was a systematically better fit with elastic scattering observables across a wide range of stable spin-0 nuclei.

For two of the structure calculations, the DH and the FZ4, we added a mean field consistently. If we used a DH structure model then we used the same DH model to simulate our mean field; likewise, this was also done using the FZ4 structure model. Overall the effects of adding this mean field to the ^{6}He and ^{8}He calculations of elastic scattering observables were smaller than seen previously for other nuclei.

In Fig. 7, we compare two calculations of ^{8}He elastically scattering off a proton at 66 MeV. Both calculations use the DH structure calculation and the Nijmegen I interaction. The difference is that the solid line sets the mean field to zero, while the dashed line includes it. For comparison, in Fig. 8, the same calculation is done using the FZ4 structure calculation and mean field using the

same FZ4 model. Both calculations give the same results: when the medium effect is added, it systematically lowers the differential cross section slightly. In general, the effect is smaller than for larger spin-0 nuclei previously studied [32,33,35]. Since these are smaller nuclei, and less tightly bound, this conclusion seems reasonable. However, it is important to note that this small change did not lead to a better description of the experimental data, in contrast to earlier work with other nuclei where there was a systematic improvement.

At higher energies, these trends continue, although their effects are smaller. We plot in Fig. 9 the elastic observables of ^{8}He at an energy of 100 MeV colliding with a proton. As in Fig. 7, the solid line represents the DH calculation without mean field effects, while the dashed line includes the effects. Both calculations use the Nijmegen I potential. These medium effects are barely discernible at this higher energy. This trend has been seen before in earlier work with other nuclei [32,33]. For complete-
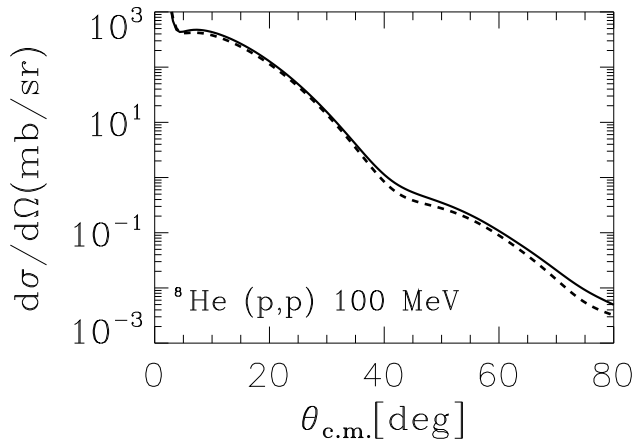
FIG. 10. Same as Fig. 8, except that now the reaction is at 100 MeV laboratory energy. There is no data for this reaction.

ness, in Fig. 10 we have calculated the same reaction as Fig. 9 except we now use the FZ4 structure calculation and mean field (dashed line) for ^{8}He. The same conclusions are reached. By using two different models, we conclude that this mean field procedure leads to results that are model independent and smaller than doubly magic nuclei at the same energies.

IV. SUMMARY AND CONCLUSION

We have presented sensitivity tests for elastic scattering observables of protons bombarded with ^{6}He and ^{8}He. Here, we found that elastic scattering is a weak tool for determining the structure of these isotopes. These conclusions were drawn by using four different nuclear structure models that had different spatial characteristics in the calculation of the proton-nucleus optical potential. All calculations using these structure models were in good agreement with the data that exist. In fact, the models not designed for exotic nuclei (Dirac-Hartree and chiral models) did as well as, and sometimes slightly better than their made-for-exotic-nuclei counter parts (COSMA and a simple 'boot-strap' model). We agree with the results of earlier work of Korsheninnikov *et al.* [11,12]. They believe that the size of the core plays a more important role in determining the differential cross section than the lower density valance neutrons. The only potential area for significant nuclear structure sensitivity with elastic scattering is with the large angle ($> 70^o$) spin observables. Since the radioactive beams are secondary beams, to produce enough polarized statistics to measure these reactions with any accuracy is beyond experimental and theoretical capabilities at the present time. It is, therefore, possible to conclude that one should look beyond intermediate elastic reactions when trying to determine the structure of the neutron rich helium isotopes. Higher energy elastic scattering (> 500 MeV/nucleon) [4] has had some success in

determining structure, although they warn against using an optical model approach, as used here [40]. Inelastic hadron reactions [41] (momentum distributions following fragmentation [16,42,43], transfer reactions [44], Coulomb breakup [45,46], excitation [47], and charged pion photo production [48]) and an interesting concept using electron scattering [14] offer hope as tools to determine conclusively the structure of ^{6}He and ^{8}He.

[1] A. A. Korsheninnikov *et al.*, Phys. Rev. C **53**, R537 (1996).
[2] A. A. Korsheninnikov *et al.*, Phys. Lett B. **316**, 38 (1993).
[3] T. T. S. Kuo, F. Krmpotić, and Y. Tzeng, Phys. Rev. Lett. **78**, 2708 (1997).
[4] J. S. Al-Khalili and J. A. Tostevin, Phys. Rev. C **57**, 1846 (1998).
[5] L. V. Chulkov, C. A. Bertulani, and A. A. Korsheninnikov, Nucl. Phys. A **587**, 291 (1995).
[6] F. A. Gareev *et al.*, EuroPhys. Lett. **20**, 487 (1992).
[7] F. A. Gareev *et al.*, Phys. Atom. Nucl. **58**, 620 (1995).
[8] S. A. Goncharov and A. A. Korsheninnikov, Phys. Atom. Nucl. **58**, 1311 (1995).
[9] M. D. Cortina-Gil *et al.*, Nucl. Phys. A **616**, 215c (1997).
[10] C. A. Bertulani and H. Sagawa, Nucl. Phys. A **588**, 667 (1995).
[11] A. A. Korsheninnikov *et al.*, Nucl. Phys. A **616**, 189 (1997).
[12] A. A. Korsheninnkov *et al.*, Nucl. Phys. A **617**, 45 (1997).
[13] S. Karataglidis, P. J. Dortmans, K. Amos, and C. Bennhold, nucl-th **9811045 (submitted to Phys. Rev C)**, (1998).
[14] E. Garrido and E. M. de Guerra, Nucl. Phys. A **650**, 387 (1999).
[15] E. Garrido, D. V. Fedorov, and A. S. Jensen, Nucl. Phys. A **650**, 247 (1999).
[16] E. Garrido, D. V. Fedorov, and A. S. Jensen, Europhys. Lett. **43**, 386 (1998).
[17] J. Wurzer and H. M. Hofmann, Phys. Rev. C **55**, 688 (1997).

[18] E. Hiyama and M. Kamimura, Nucl. Phys. A **588**, 35c (1995).

[19] K. Varga, Y. Suzuki, and Y. Ohbayasi, Phys. Rev. C **50**, 189 (1994).

[20] M. V. Zhukov *et al.*, Phys. Rep. **231**, 152 (1993).

[21] M. V. Zhukov, A. A. Korsheninnikov, and M. H. Smedberg, Phys. Rev. C **50**, R1 (1994).

[22] A. Corbis, D. V. Fedorov, and A. S. Jensen, Phys. Rev. Lett. **79**, 2411 (1997).

[23] K. Kaki and S. Hirenzaki, Int. J. Mod. Phys. E **8**, 167 (1999).

[24] C. Elster, S. P. Weppner, and C. R. Chinn, Phys. Rev C **56**, 2080 (1997).

[25] S. P. Weppner, Ph.D. thesis, Ohio University, 1997.

[26] R. Sherr, Phys. Rev. C **54**, 1177 (1996).

[27] J. J. Rusnak and R. J. Furnstahl, Nucl. Phys. A **627**, 495 (1997).

[28] R. J. Furnstahl, B. D. Serot, and H. B. Tang, Nucl. Phys. A **615**, 441 (1997).

[29] B. C. Clark *et al.*, Phys. Lett. B **427**, 231 (1998).

[30] C. J. Horowitz and B. D. Serot, Nucl. Phys. A **368**, 503 (1981).

[31] C. J. Horowitz, D. P. Murdoch, and B. D. Serot, in *Computational Nuclear Physics 1*, edited by K. Langanke, J. A. Maruhn, and S. E. Koonin (Springer-Verlag, Berlin, 1991).

[32] C. R. Chinn, C. Elster, R. M. Thaler, and S. P. Weppner, Phys. Rev. C **52**, 1992 (1995).

[33] C. R. Chinn, C. Elster, and R. M. Thaler, Phys. Rev. C **48**, 2956 (1993).

[34] C. Elster and S. P. Weppner, Phy. Rev. C **57**, 189 (1998).

[35] C. R. Chinn, C. Elster, R. M. Thaler, and S. P. Weppner, Phys. Rev. C **51**, 1418 (1995).

[36] R. Crespo, J. A. Tostevin, and R. C. Johnson, Phys. Rev. C **51**, 3283 (1995).

[37] E. Garrido, D. V. Fedorov, and A. S. Jensen, Nucl. Phys. A **617**, 153 (1997).

[38] V. G. Stokes, R. A. M. Klamp, C. P. F. Terheggan, and J. J. de Swart, Phys. Rev. C **49**, 2950 (1994).

[39] R. Machleidt, F. Sammarruca, and Y. Song, Phys. Rev. C **53**, R1483 (1996).

[40] R. Crespo and R. C. Johnson, Phys. Rev. C **60**, 034007 (1999).

[41] I. J. Thompson, J. Phys. G **23**, 1245 (1997).

[42] I. Tanihata *et al.*, Phys. Lett. B **289**, 261 (1992).

[43] M. V. Zhukov, A. A. Korsheninnikov, M. H. Smedberg, and T. Kobayashi, Nucl. Phys. A **583**, 803 (1995).

[44] S. N. Ershov *et al.*, Phys. Rev. C **56**, 1483 (1997).

[45] F. M. Numes and I. J. Thompson, Phys. Rev. C **59**, 2652 (1999).

[46] R. Shyam and I. J. Thompson, Phys. Rev. C **59**, 2645 (1999).

[47] B. V. Danilin *et al.*, Phys. Rev. C **55**, R577 (1997).

[48] S. Karataglidis and C. Bennhold, Phys. Rev. Lett. **80**, 1614 (1998).